

ValID: Verification as Late Integration of Detections for LiDAR-Camera Fusion

Vanshika Vats*, Marzia Binta Nizam* and James Davis

Abstract— Vehicle object detection benefits from both LiDAR and camera data, with LiDAR offering superior performance in many scenarios. Fusion of these modalities further enhances accuracy, but existing methods often introduce complexity or dataset-specific dependencies. In our study, we propose a model-adaptive late-fusion method, VaLID, which validates whether each predicted bounding box is acceptable or not. Our method verifies the higher-performing, yet overly optimistic LiDAR model detections using camera detections that are obtained from either specially trained, general, or open-vocabulary models. VaLID uses a simple multi-layer perceptron trained with a high recall bias to reduce the false predictions made by the LiDAR detector, while still preserving the true ones. Evaluating with multiple combinations of LiDAR and camera detectors on the KITTI dataset, we reduce false positives by an average of 63.9%, thus outperforming the individual detectors on 3D average precision (3DAP). Our approach is model-adaptive and demonstrates state-of-the-art competitive performance even when using generic camera detectors that were not trained specifically for this dataset.

I. INTRODUCTION

The development of autonomous vehicles relies heavily on accurate object detection to safely navigate their environment. These systems use multiple sensors, such as cameras and LiDAR, each offering unique strengths and weaknesses. Cameras provide detailed visual information, while LiDAR offers precise depth information crucial for 3D localization. While systems using only cameras or LiDAR data provide valuable information, single-sensor approaches often fail. Cameras struggle in low-light conditions [5], [23], and LiDAR lacks rich high resolution visual data [12], [27], [33], [52].

Multi-modal fusion is often used to ensure robust and reliable detection [37], [38]. These methods combine LiDAR’s depth data with camera visuals to create a more reliable detection system. However, the integration of these modalities often requires advanced fusion techniques with methods designed to match the specific characteristics of the underlying data [1], [10], [41], [51]. The primary challenge is ensuring that the strengths of each modality complement one another to improve overall detection accuracy in varied and dynamic driving conditions.

Sensor fusion in autonomous vehicles can be categorized into early, deep, and late fusion techniques. Early fusion integrates raw data from multiple sensors early in the processing

pipeline, allowing for detailed cross-sensor interaction [35], [48]. However, this approach can lead to increased computational costs due to the need for complex preprocessing steps, like semantic segmentation or depth completion [7], [43], [46]. Deep fusion aligns features at a higher abstraction level, balancing information from both sensors but adding complexity to the model design [20], [36]. Late fusion, in contrast, merges detection outputs at the bounding box level after independent processing, offering more flexibility and computational efficiency but with reduced feature interaction [25], [26].

Early and deep fusion methods leverage cross-modality information in their fundamental representations, potentially leading to higher accuracy at the cost of complexity. Late fusion methods, on the other hand, are simpler to integrate into complex industrial workflows, since they do not require a redesign when advances are made in underlying detection technologies. Pre-trained single-modality detectors can be used and replaced without modification, requiring only detection-level outputs at the time of fusion. An ideal fusion method would allow the flexibility of late-fusion while obtaining the performance of early and deep fusion.

We introduce a new late fusion method called VaLID: Verification as Late Integration of Detections. This method takes raw detections from a LiDAR model and cross-validates them against corresponding camera detections using a simple multi-layer perceptron neural network. Ensuring that only verified LiDAR boxes are kept significantly reduces false positives, improving overall performance.

We evaluate our method on the KITTI dataset with two LiDAR detectors, PV-RCNN [32] and TED-S [42]. To ensure generality, we use three distinct camera models: MonoDETR [49] is a special purpose detector trained specifically on KITTI, YOLO-NAS is a general-purpose model from the YOLO [30] family, and Grounding DINO [16] is an open-vocabulary model.

Detection methods trained for a specific dataset normally outperform general purpose models. Our two LiDAR methods were selected as state-of-the-art methods designed and tested on the KITTI dataset. For camera detectors we included general purpose detectors in our evaluation. These have lower performance than a specialized model when considered as a primary detector, however our method uses camera models for the easier task of verification.

We find that the VaLID method removes an average 63.9% of false positives, consistently improving overall detection average precision. Importantly, improvement is as effective using the general camera models as it is with the specifically

* Authors contributed equally

Vanshika Vats, Marzia Binta Nizam, and James Davis are with the Department of Computer Science and Engineering, University of California Santa Cruz, Santa Cruz, CA 95064, USA (vvats, manizam, davisje)@ucsc.edu



Fig. 1: We conduct our study on the KITTI dataset. The figure rows show (a) official 2D ground truth (b) detections from the specialized LiDAR model PVRCCNN, (c) specialized camera model MonoDETR, and (d) open Vocabulary model GroundingDino. LiDAR generally produces too many false positives, seen most obviously in Column [i]. Camera models can help verify and reject false positives despite imperfections in their own detections (e.g. Missed detection of partial car in Row[c]Col[ii], and Imperfect dimensions in Row[d]Col[iii]).

trained method. In both cases, results are competitive with the state of the art.

Thus, the primary contributions of our work are:

- We propose VaLiD, a lightweight, model-adaptive late-fusion approach that focuses on reducing false positives by cross-validating them with camera detections.
- Our method works with both specialized and general-purpose camera models without requiring individual model retraining or dataset-specific fine-tuning, making it adaptable to various detection backbones.
- Our method uses a multi-layered perceptron (MLP) with confidence rescoreing that balances simplicity and effectiveness, avoiding the complexity of deep-fusion methods while achieving competitive performance.

II. RELATED WORK

A. Detection Using Camera Images

Cameras images are fundamentally a 2D data source, and 2D object detection is a well-studied area with many surveys and general purpose datasets [6], [15]–[17], [21], [29], [31], [39], [53]. Higher accuracy is possible in specific domains such as vehicle detection by designing specialized object detection methods which are trained on vehicle specific datasets [3], [8], [34]. Since autonomous driving requires 3D awareness, there have also been attempts to detect 3D bounding boxes from camera images. However, accurately estimating depth without dedicated sensors is challenging, especially for distant objects. Early approaches like Deep3DBox leverage 2D bounding boxes and geometric constraints to infer 3D dimensions but struggle with long-range accuracy [23]. Similarly, MonoDETR improves detection by incorporating depth embeddings into a transformer

model [49]. Other methods generate depth maps to assist with detection. For instance, MonoPGC refines pixel-wise depth estimation through cross-attention [45], and Pseudo-LiDAR simulates LiDAR input from depth maps to enhance detection performance [40]. While these techniques improve depth accuracy, they often introduce significant computational overhead, especially for complex or occluded scenes. Multi-task approaches like Deep MANTA predict both 2D and 3D attributes simultaneously, leveraging shared features to enhance efficiency, but they still face challenges in reliable depth estimation [5]. Unfortunately, camera-only methods, while effective in some scenarios, are limited by their inability to produce reliable depth estimation without additional sensors, and 3D bounding box accuracy remains below 2D bounding box accuracy. In our work, we use the higher accuracy 2D detections from camera images as one of the inputs to our late fusion method, which integrates data from multiple sensors.

B. Detection Using LiDAR Point Clouds

LiDAR-based 3D detection has become a fundamental component in autonomous driving due to its ability to capture detailed spatial information. One-stage models, like PointNet and PointNet++, were early efforts that applied neural networks directly to raw point clouds [27], [28]. These methods prioritized real-time processing but often struggled with long-range accuracy. Other approaches, like those using range images, attempt to enhance detection by encoding depth information at the pixel level, yet they still face limitations in handling complex, distant scenes [22], [2]. To address these challenges, two-stage models were developed to refine detection for better accuracy. VoxelNet [52] and SECOND [47] introduced the use of 3D voxels and

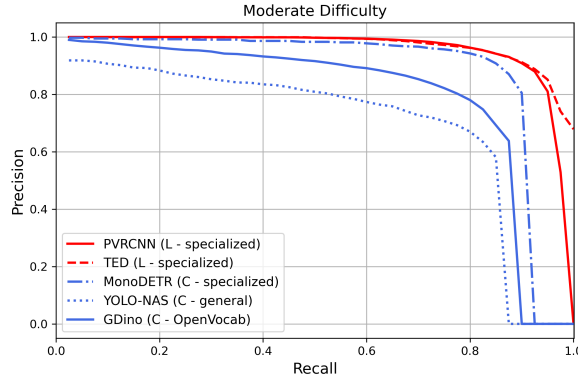


Fig. 2: Precision-Recall curve (PRC) of our baseline single modality models on the KITTI moderate difficulty data set. Notice that both LiDAR models outperform all three of the camera models and that the specialized camera detector outperforms the two general-purpose camera-based object detectors.

sparse convolutions, enhancing both feature extraction and processing efficiency. Building on this, PV-RCNN combines voxel-based CNNs with PointNet abstraction to generate high-quality 3D proposals [32], while PointRCNN [33] refines 3D proposals in a two-stage process. Part-A2Net [32] goes a step further by predicting part locations within objects to refine proposals, improving 3D bounding box accuracy. LiDAR-only methods offer robust spatial data but often struggle with complex environments and distant objects. In our late fusion approach, LiDAR detections are combined with camera detections to provide more accurate and reliable 3D object detection.

C. Detection Using LiDAR-Camera Fusion

Multi-modal fusion techniques for 3D detection are increasingly common, particularly in autonomous driving, where camera and LiDAR sensors complement each other. These techniques are categorized into three main approaches: early, deep, and late fusion.

Early fusion methods integrate camera data with LiDAR point clouds early in the perception pipeline to enhance object detection. Techniques like PointPainting and MVP enrich LiDAR data by projecting 2D camera segmentation or generating virtual points to address LiDAR sparsity in distant regions [35], [48]. However, image-based segmentation can blur object boundaries, a problem mitigated by FusionPainting using 3D segmentation [46]. Techniques like VirConv create virtual points and apply Stochastic Voxel Discard to filter noise, though this adds computational overhead [7], [43].

Deep fusion methods operate at a higher level of abstraction, aligning features from both modalities. Models like PointAugmenting and DVF bridge the 2D-3D gap by projecting point clouds onto image feature maps or reweighting voxel features based on pixel confidence [20], [36]. Advanced models such as EPNet, EPNet++, and DeepFusion use attention mechanisms to dynamically adjust feature weights, reducing inconsistencies [11], [14], [18]. SFD addresses information loss by fusing features directly in the 3D Region of Interest (RoI), while BEVFusion unifies features

into a Bird’s Eye View (BEV) representation [19], [44].

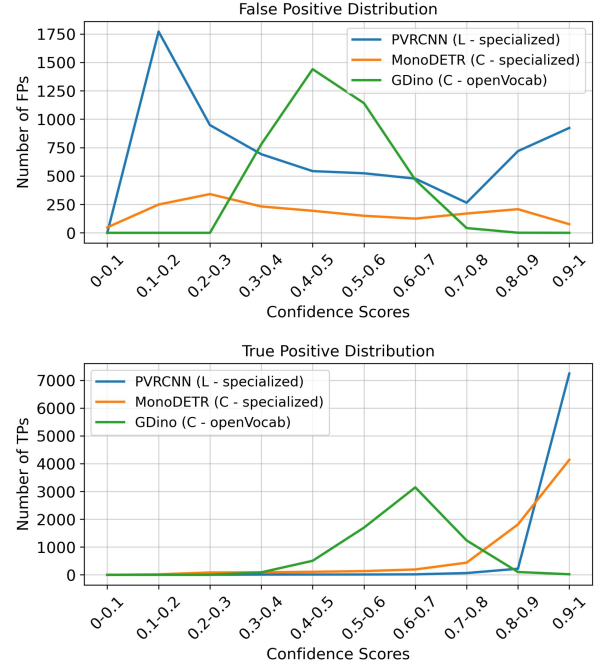


Fig. 3: The distribution of false positives and true positives across confidence score bands for one LiDAR and two camera object detection models on the KITTI moderate set. Notice that the LiDAR method has false positives across all confidence bands, and that the camera methods have different and sometimes complementary distributions.

Late fusion integrates outputs from each sensor after independent processing. For example, CLOCs and Fast-CLOCs refine detection confidence by ensuring that 2D and 3D bounding boxes overlap accurately, but these methods primarily focus on raw data from each sensor [25], [26]. They use Multi-Layer Perceptrons (MLP) to process detection candidates, but insufficient feature alignment can result in suboptimal training performance. C-CLOCs addresses this limitation by incorporating contrastive learning and aligning features from both 2D and 3D sensors to improve detection accuracy, particularly in challenging environments [50]. Çaldırın and Acarman take a different approach, integrating 2D segmentation with 3D LiDAR to reduce false positives, such as roadblocks and tunnel walls, improving detection accuracy [4]. All of these late-fusion methods for vehicle detection have focused on combining specialized LiDAR and camera vehicle detectors.

Our work proposes a new late fusion method that is competitive with the state of the art. We demonstrate results with both a specialized camera detector trained on the KITTI dataset and with more general vision models that lack specific knowledge of the dataset.

III. BACKGROUND

A. LiDAR and Camera Models for Late-Fusion

Many urban driving object detection methods utilize LiDAR and camera modalities separately, as well as in fusion, for enhanced performance. Most methods, however,

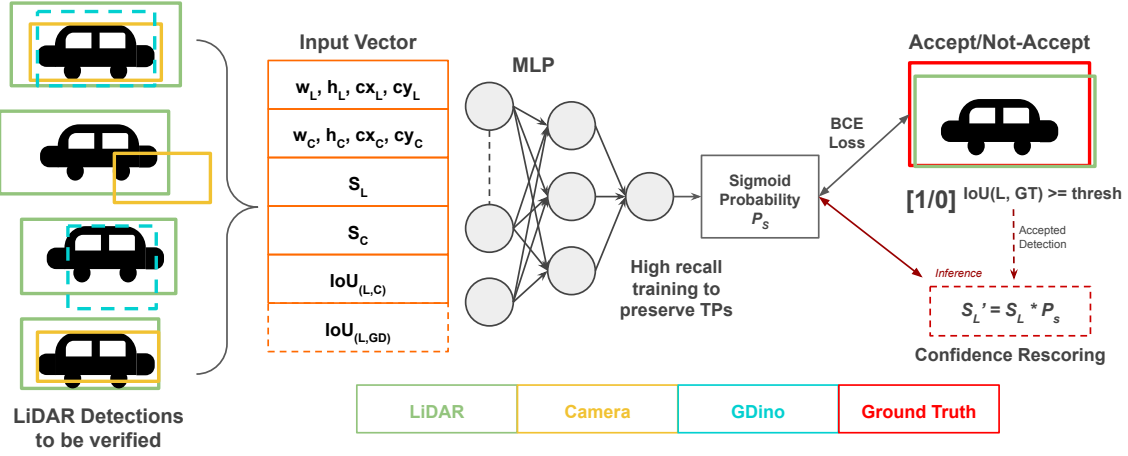


Fig. 4: In our method called VaLiD, we take LiDAR (L) boxes as the primary detections and use the camera (C) modality to verify whether each L box is an acceptable detection or not. The input vector is given as the bounding box dimensions of width w , height h , and center (cx, cy) , confidence scores s , and the measure of overlap IoU . We pass this vector through an MLP and output an accept or reject signal as a sigmoid value. The target loss is calculated considering the overlap of the ground truth with the given L box. During the inference, the accepted box confidence is rescored by multiplying it with the output sigmoid probability in order to reduce the confidence of the lingering false positives.

use specialized training and fine-tuning tailored to specific datasets, which is both time-consuming and computationally demanding. To reduce this dependency, our study leverages general and open-vocabulary camera models without requiring dataset-specific fine-tuning. We perform our study on the KITTI dataset [8], using PVRCNN [32] and TED-S [42] models as the primary LiDAR models. For fusion, we use MonoDETR [49] as a specialized KITTI model, and YOLO-NAS [30] as a general camera detector that is not trained on KITTI. GroundingDINO [16] is used as an open-vocabulary model that can detect objects that are not even seen during the training. Although not as precise as fine-tuned models, these general models offer cross-domain versatility, providing the flexibility needed for a more robust late-fusion approach.

B. Model Detections Complement Each Other

LiDAR and camera models have their own strengths and weaknesses. Fig. 1 illustrates how these models, while missing certain detections, often compensate for one another's limitations. For instance, PVRCNN can identify numerous objects but tends to generate a lot of false positives. Meanwhile, MonoDETR and GroundingDINO may miss some detections covered by PVRCNN, but they also detect objects that PVRCNN overlooks. GroundingDINO, despite producing imperfect bounding boxes and some false positives, detects objects that specialized models may miss.

Fig. 2 shows the overall performance of our baseline LiDAR and camera methods. Notice that both LiDAR methods outperform all three camera methods, and that the specialized camera model outperforms the two general models. Since the LiDAR methods outperform the camera methods, we take them as our primary detectors and use the camera methods to augment their detection ability.

Unfortunately, the tested LiDAR methods produce many false positives which negatively impacts the overall system performance. Reducing these false positives is crucial for

enhancing precision. To better understand the distribution of false positives, Fig. 3 shows false positives and true positives over different confidence bands for several methods. Notice that the overall distributions are different in different methods. The neural network in our fusion model learns to leverage these differences.

IV. DESIGN AND IMPLEMENTATION

A. Method Overview

We use camera model detections and a neural network to verify whether a particular LiDAR bounding box detection is valid. Fig. 4 provides an overview of our method. For each LiDAR detection, we look for a corresponding camera detection in which the overlap score (IoU) is 0.5 or higher. This threshold is intentionally set lower than the official KITTI benchmark of 0.7 to account for potential inaccuracies in the camera detection dimensions, ensuring that valid detections are not inadvertently discarded due to minor misalignments. If a matching camera box is found, the camera bounding box, the Intersection over Union (IoU) between the LiDAR and camera boxes, and the confidence scores of both detections are fed into a neural network, along with the LiDAR box. If no matching camera box is found, we input a zero for both the bounding box and the confidence score for the camera model. The inputs given would be:

$$I = \{Bbox_L, Bbox_C, S_L, S_C, IoU_{(L,C)}, [IoU_{(L,GT)}]\} \quad (1)$$

where $Bbox_L$ and $Bbox_C$ are the dimensions of bounding boxes of LiDAR and camera models respectively, represented by their width, height, and center coordinates, normalized by the image's dimensions. S_L and S_C are their confidence scores, and $IoU_{(L,C)}$ is the Intersection over Union of LiDAR and camera detection. When two camera methods are used, information about a second bounding box is provided. For example, $IoU_{(L,GT)}$ is the optionally provided IoU between LiDAR and GroundingDINO.

Models	Modality	Easy		Hard	
		TP	FP	TP	FP
PVRCNN	L	1433	1287	5364	3620
PV+Mono (Ours)	LC	1428	393	5280	1084
PV+YOLO (Ours)	LC	1430	360	5278	965
PV+GDino (Ours)	LC	1430	366	5271	937
PV+Mono+GDino (Ours)	LCC	1430	354	5261	906
PV+YOLO+GDino (Ours)	LCC	1430	347	5266	887
TED	L	1434	864	5425	1848
TED+Mono (Ours)	LC	1434	323	5210	599
TED+YOLO (Ours)	LC	1434	389	5380	1028
TED+GDino (Ours)	LC	1434	352	5359	869
TED+Mono+GDino (Ours)	LCC	1434	334	5343	826
TED+YOLO+GDino (Ours)	LCC	1434	381	5354	914

TABLE I: Since ours is a late fusion method that generates no new detections, we focus on reducing false positives (FPs) while preserving true positives (TPs). Our method is successfully able to do so, reducing the FPs by an average of 73.6% on PVRCNN and 54.2% on TED.

Our goal is to determine whether to keep or discard each LiDAR (L) detection. We generate ground truth by calculating the IoU between the LiDAR box and the official KITTI ground truth, and follow the dataset’s standard by setting an IoU threshold of 0.7 for the *Car* class. Detections above this threshold are marked as valid (positive class), while those below are ignored.

Validating LiDAR detections with camera detections could be approached with a simple thresholding heuristics. However, simple heuristics would fail to capture the complex, non-linear relationships between LiDAR and camera detections, such as bounding boxes with high confidence but low IoU or cases where one modality compensates for the other. A neural network allows this relationship to be learned from the data, rather than hand tweaked by the researcher for each new pair of detectors. Given the small, fixed-size feature vector in a structured format, an MLP is an efficient and effective choice. It can learn non-linear patterns and adapt to biases in false positives across different parametric bands, which are not the same in different detection models (Fig. 3). More complex models like CNNs or transformers, designed for high-dimensional inputs, would add unnecessary complexity without offering meaningful improvements.

The input vector I (Eq. 1) is, therefore, fed to a two-layered MLP that is specifically designed to address the tradeoff between preserving true positives and reducing false positives. The MLP is trained with a high recall bias to minimize the risk of mistakenly discarding true positive detections while effectively filtering out false positives. This MLP is simple and architecturally identical in all of our experiments. However, the activation weights need to be trained for each pair of LiDAR and camera methods since each baseline method has its own distributions of true and false positives, and the goal of the MLP is to make specific tradeoffs in these distributions.

To ensure that enough verification boxes exist, we desire an over-production of bounding boxes in the camera-based verification methods as opposed to under-production, and thus include even boxes with low confidence. We observe

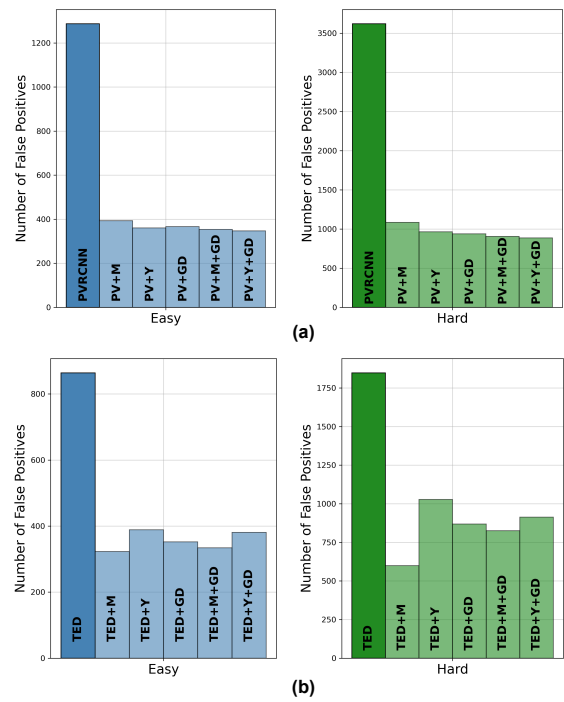


Fig. 5: Our fusion method is able to reduce the false positives significantly on (a) PVRCNN, and (b) TED model detections. Note that this improvement is achieved for all tested camera methods used for verification.

that the open vocabulary camera model provides detected boxes that are not as precisely aligned as the specialized LiDAR and camera models, especially around occluded objects, and thus adjust the IoU threshold to ensure sufficient matching boxes exist.

Since we employ high-recall training, we expect some false positives will continue to be accepted by the MLP during inference. To mitigate their impact on the overall average precision (AP), we assign a final confidence (S'_L) to each box by multiplying the accepted LiDAR box confidence score S_L with the predicted output sigmoid probability P_S . This ensures that true positive boxes retain high confidence, while false positives with lower predicted probabilities are down-weighted, effectively balancing the AP.

B. Implementation

To implement our late-fusion method, we combine two specialized LiDAR detectors (PVRCNN and TED) with various camera models: a specialized model (MonoDETR), a general-purpose model (YOLO-NAS), and an open-vocabulary model (GroundingDINO). The experiments are conducted on the KITTI dataset. We remove dataset images for which ground truth is not available, as well as those that have already been used to train our baseline models. This leaves 3769 images available for our experiments comprising the subset that the dataset providers call validation. We split these images into training and testing subsets. For PVRCNN, these images generate a training set of 12,303 LiDAR bounding box samples and test set of 12,817 bounding boxes. For TED-S, we obtain 9,016 training and 9,406 testing bounding boxes.

Models	Modality	Model Type	3D AP / 2D AP (%)		
			Easy	Moderate	Hard
MonoDETR [49]	C	Specialized	28.05 / 95.12	20.77 / 87.36	17.43 / 79.94
YOLO-NAS [30]	C	General	N/A / 75.32	N/A / 68.69	N/A / 55.11
GroundingDino [16]	C	Open-Vocab	N/A / 84.73	N/A / 78.68	N/A / 62.82
PVRCNN [32]	L	Specialized	91.94 / 98.30	82.97 / 94.44	82.44 / 94.08
Ours (<i>PVRCNN+MonoDETR</i>)	LC	Late-Fusion	91.96 / 98.91	83.47 / 95.45	82.89 / 93.11
Ours (<i>PVRCNN+YOLO-NAS</i>)	LC	Late-Fusion	92.30 / 99.09	83.83 / 95.83	82.91 / 93.33
Ours (<i>PVRCNN+GDino</i>)	LC	Late-Fusion	92.41 / 98.91	83.54 / 95.26	83.01 / 93.01
Ours (<i>PVRCNN+MonoDETR+GDino</i>)	LCC	Late-Fusion	92.37 / 99.15	83.91 / 95.87	83.08 / 93.37
Ours (<i>PVRCNN+YOLO-NAS+GDino</i>)	LCC	Late-Fusion	92.46 / 99.24	83.93 / 95.99	82.95 / 93.42
TED-S [42]	L	Specialized	95.23 / 98.88	87.98 / 96.73	86.28 / 94.95
Ours (<i>TED+MonoDETR</i>)	LC	Late-Fusion	95.40 / 99.23	88.69 / 95.64	86.77 / 95.59
Ours (<i>TED+YOLO-NAS</i>)	LC	Late-Fusion	95.18 / 99.12	88.73 / 95.79	86.64 / 95.66
Ours (<i>TED+GDino</i>)	LC	Late-Fusion	95.86 / 99.35	88.85 / 95.69	86.78 / 95.57
Ours (<i>TED+MonoDETR+GDino</i>)	LCC	Late-Fusion	95.59 / 99.40	88.94 / 95.93	86.80 / 95.74
Ours (<i>TED+YOLO-NAS+GDino</i>)	LCC	Late-Fusion	95.38 / 99.19	88.78 / 95.87	86.83 / 95.70
CLOCs [25]	LC	Late-Fusion	92.74 / 99.33	82.90 / 93.75	77.75 / 92.89
CMKD [9]	C(+L)	Knowledge Distil.	34.56 / 96.08	23.10 / 92.43	19.52 / 87.11
LogoNet [13]	LC	Deep Fusion	92.04 / 97.04	85.04 / 89.44	84.31 / 89.20

TABLE II: Performance on the Average Precision (AP) metric for our method on all difficulty sets on KITTI-val for the *Car* class. In general, the baseline camera methods do not produce 3D bounding boxes (N/A) or produce ones with very low performance (MonoDETR). Our late fusion method consistently outperforms the original specialized LiDAR and camera methods in 3DAP across all the difficulty levels. Our method is also comparable to the SOTA deep fusion methods, despite being simpler and lightweight, without requiring special integrated training on the individual models. The color coding in yellow emphasizes the degree of improvement on 3DAP (primary comparison metric) over the baselines.

The final inputs to our model include details such as LiDAR bounding box dimensions, confidence scores, and IoUs from the camera methods. These inputs pass through a two-layer multi-layer perceptron with ReLU [24] activation function and a last sigmoid layer. This output decides whether to keep each LiDAR box or discard the detection. Since our focus is on reducing false positives without significantly disturbing the true positive count, we use class weights of 1:10 for negative and positive classes to maintain high recall. The model is optimized using a binary cross-entropy loss function, which compares the sigmoid outputs against the ground truth labels to predict the acceptance or rejection of a given LiDAR detection. We train our models for 50 epochs with an Adam learning rate of 0.0001. During the inference time, we rescore the accepted LiDAR box confidence score by multiplying it by the output sigmoid prediction probability, refining the final detection confidence.

V. RESULTS

We present the results of our methods in two parts: First, we show the impact of our fusion method on reducing false positives generated by LiDAR-only models. Second, we provide an overall comparison of the Average Precision (3D/2DAP), comparing our fusion method with single-modality models as well as state-of-the-art fusion methods.

A. False Positives Reduction

Table I shows the performance of LiDAR-only models in terms of true positive and false positive bounding box predictions. Note that both LiDAR models produce a large number of false positives. Our late fusion method is evaluated on each LiDAR model, using each of our three baseline camera detectors, as well as using combinations of camera detectors. Our method consistently and substantially reduces false positives across all combinations. This is made especially clear through the visualization in Figure 5. Our late fusion method achieves an average false positive reduction of 73.6% on PVRCNN and 54.2% on TED. Importantly, the true positive (TP) numbers have only a small reduction, indicating that the significant decrease in false positives does not come at the cost of many missed detections. The results are qualitatively shown in Figure 6.

B. Average Precision

Table II presents the Average Precision (AP) for 3D object detection across the *Easy*, *Moderate*, and *Hard* KITTI sets on the *Car* class, comparing individual LiDAR models, camera models, and their fusion combinations. Our late fusion method shows consistently improved performance compared to any single-modality models, outperforming PV-RCNN and TED-S in 3D AP. The median improvement is +0.52 across all 3D-AP tests and difficulty levels, with an interquartile range of +0.43 to +0.86. While this improvement is modest,



Fig. 6: Qualitative results illustrating the reduction of false positives from our fusion method as compared to the specialized LiDAR PVRCNN. (a) denotes the ground truth bounding boxes in the KITTI-val set. In (b), red boxes represent the false positives generated by PVRCNN, while green boxes indicate the final accepted boxes from our late fusion method, demonstrating a significant decrease in false positives.

Models	Modality	Model Type	3D AP / 2D AP (%)		
			Easy	Moderate	Hard
PVRCNN [32]	L	Specialized	64.25 / 72.00	57.00 / 66.58	52.00 / 63.34
Ours (PVRCNN+YOLO-NAS)	LC	Late-Fusion	67.09 / 73.54	59.79 / 68.57	53.74 / 64.69
Ours (PVRCNN+GDino)	LC	Late-Fusion	65.64 / 72.02	58.42 / 67.30	52.82 / 63.42
Ours (PVRCNN+YOLO-NAS+GDino)	LC	Late-Fusion	67.28 / 73.97	60.36 / 68.01	54.31 / 63.58

TABLE III: Performance on the Average Precision (AP) metric for our method on all difficulty sets on KITTI-val for the *Pedestrian* class. Our late fusion method consistently outperforms the original specialized methods in 3DAP across all the difficulty levels. The color coding in yellow emphasizes the degree of improvement on 3DAP (primary comparison metric) over the baselines.

the performance on this dataset is already near saturation, leaving very little margin for error reduction. Hence, modest gains like this are typical of current state-of-the-art methods on KITTI for the *Car* class. To verify the generalizability of our method, we evaluate it on the *Pedestrian* class using models for which labels were available (Table III). Given a larger scope of error reduction for this class, we see that our fusion method demonstrates a median improvement of +2.31 with an interquartile range of +1.40 to +2.93 across all difficult levels.

Late fusion with general and open-vocabulary camera models (YOLO-NAS and GroundingDINO) perform as well as the tested special-purpose camera model (MonoDETR). This is surprising since the baseline AP of these detectors is much lower than the specially trained model. This provides evidence that general-purpose camera detectors can be used to enhance special-purpose LiDAR detectors.

Although our primary goal is to show that our late fusion method improves scores relative to the baseline methods, the table also provides numbers for comparison fusion methods. Our approach provides higher scores using a simpler method.

VI. LIMITATIONS

Our late fusion method is targeted at reducing false positives, but does not seek to increase true positives. We thus

require that the LiDAR (or primary) detector successfully finds most true positives. Similarly, since our approach relies on validating LiDAR detections with camera inputs, it may not perform well with camera models that produce few detections and is, therefore, more applicable to methods that can be tuned for a greater number.

VII. CONCLUSION

In this paper, we propose a model-adaptable late fusion method that combines LiDAR and camera detections to enhance object detection performance for autonomous vehicles. Our approach focuses on reducing false positives by cross-validating LiDAR detections with camera inputs. Experiments on the KITTI dataset demonstrate that our method is exceptional at its primary goal of reducing false positives, and provides modest but consistent improvements in average precision. The method performs competitively with state-of-the-art comparison methods.

Importantly, the method works equally well with relatively low precision general purpose camera detectors which were not specifically trained on this dataset or for these specific detection classes. This is a surprising result, which we hope sparks future research on using general-purpose 2D detectors to improve the special purpose 3D vehicle detectors which currently dominate the state of the art.

ACKNOWLEDGMENTS

Partial support to some authors for this work was provided by WISEautomotive through the ATC+ Program award from MOTIE Korea 20014264.

REFERENCES

- [1] Eduardo Arnold, Omar Y Al-Jarrah, Mehrdad Dianati, Saber Fallah, David Oxtoby, and Alex Mouzakitis. A Survey on 3D Object Detection Methods for Autonomous Driving Applications. *IEEE Transactions on Intelligent Transportation Systems*, 20(10):3782–3795, 2019.
- [2] Alex Bewley, Pei Sun, Thomas Mensink, Dragomir Anguelov, and Cristian Sminchisescu. Range Conditioned Dilated Convolutions for Scale Invariant 3D Object Detection. *arXiv preprint arXiv:2005.09927*, 2020.
- [3] Holger Caesar, Varun Bankiti, Alex H Lang, Sourabh Vora, Venice Erin Liang, Qiang Xu, Anush Krishnan, Yu Pan, Giancarlo Baldan, and Oscar Beijbom. nuScenes: A Multimodal Dataset for Autonomous Driving. In *Proceedings of the IEEE/CVF conference on Computer Vision and Pattern Recognition*, pages 11621–11631, 2020.
- [4] Bekir Eren Calderin and Tankut Acarman. A Late Asymmetric Fusion Approach To Eliminate False Positives. In *2022 IEEE 25th International Conference on Intelligent Transportation Systems (ITSC)*, pages 2080–2085. IEEE, 2022.
- [5] Florian Chabot, Mohamed Chaouch, Jaonary Rabarisoa, Céline Teuliere, and Thierry Chateau. Deep MANTA: A Coarse-to-fine Many-Task Network for joint 2D and 3D vehicle analysis from monocular image. In *Proceedings of the IEEE conference on Computer Vision and Pattern Recognition*, pages 2040–2049, 2017.
- [6] Jia Deng, Wei Dong, Richard Socher, Li-Jia Li, Kai Li, and Li Fei-Fei. ImageNet: A Large-scale Hierarchical Image Database. In *2009 IEEE conference on Computer Vision and Pattern Recognition*, pages 248–255. IEEE, 2009.
- [7] Jian Dou, Jianru Xue, and Jianwu Fang. SEG-VoxelNet for 3D vehicle detection from RGB and LiDAR data. In *2019 International Conference on Robotics and Automation (ICRA)*, pages 4362–4368. IEEE, 2019.
- [8] Andreas Geiger, Philip Lenz, Christoph Stiller, and Raquel Urtasun. Vision meets Robotics: The KITTI dataset. *The International Journal of Robotics Research*, 32(11):1231–1237, 2013.
- [9] Yu Hong, Hang Dai, and Yong Ding. Cross-Modality Knowledge Distillation Network for Monocular 3D Object Detection. In *European Conference on Computer Vision*, pages 87–104. Springer, 2022.
- [10] Keli Huang, Botian Shi, Xiang Li, Xin Li, Siyuan Huang, and Yikang Li. Multi-modal Sensor Fusion for Auto Driving Perception: A Survey. *arXiv preprint arXiv:2202.02703*, 2022.
- [11] Tengteng Huang, Zhe Liu, Xiuw Chen, and Xiang Bai. EPNet: Enhancing Point Features with Image Semantics for 3D Object Detection. In *Computer Vision–ECCV 2020: 16th European Conference, Glasgow, UK, August 23–28, 2020, Proceedings, Part XV 16*, pages 35–52. Springer, 2020.
- [12] Alex H Lang, Sourabh Vora, Holger Caesar, Lubing Zhou, Jiong Yang, and Oscar Beijbom. PointPillars: Fast Encoders for Object Detection from Point Clouds. In *Proceedings of the IEEE/CVF conference on Computer Vision and Pattern Recognition*, pages 12697–12705, 2019.
- [13] Xin Li, Tao Ma, Yuenan Hou, Botian Shi, Yuchen Yang, Youquan Liu, Xingjiao Wu, Qin Chen, Yikang Li, Yu Qiao, et al. LoGoNet: Towards Accurate 3D Object Detection With Local-to-Global Cross-Modal Fusion. In *Proceedings of the IEEE/CVF Conference on Computer Vision and Pattern Recognition*, pages 17524–17534, 2023.
- [14] Yingwei Li, Adams Wei Yu, Tianjian Meng, Ben Caine, Jiquan Ngiam, Daiyi Peng, Junyang Shen, Yifeng Lu, Denny Zhou, Quoc V Le, et al. DeepFusion: LiDAR-Camera Deep Fusion for Multi-Modal 3D Object Detection. In *Proceedings of the IEEE/CVF conference on Computer Vision and Pattern Recognition*, pages 17182–17191, 2022.
- [15] Tsung-Yi Lin, Michael Maire, Serge Belongie, James Hays, Pietro Perona, Deva Ramanan, Piotr Dollár, and C Lawrence Zitnick. Microsoft COCO: Common Objects in Context. In *Computer Vision–ECCV 2014: 13th European Conference, Zurich, Switzerland, September 6–12, 2014, Proceedings, Part V 13*, pages 740–755. Springer, 2014.
- [16] Shilong Liu, Zhaoyang Zeng, Tianhe Ren, Feng Li, Hao Zhang, Jie Yang, Chunyuan Li, Jianwei Yang, Hang Su, Jun Zhu, et al. Grounding DINO: Marrying DINO with grounded pre-training for open-set Object Detection. *arXiv preprint arXiv:2303.05499*, 2023.
- [17] Wei Liu, Dragomir Anguelov, Dumitru Erhan, Christian Szegedy, Scott Reed, Cheng-Yang Fu, and Alexander C Berg. SSD: Single Shot Multibox Detector. In *Computer Vision–ECCV 2016: 14th European Conference, Amsterdam, The Netherlands, October 11–14, 2016, Proceedings, Part I 14*, pages 21–37. Springer, 2016.
- [18] Zhe Liu, Tengteng Huang, Bingling Li, Xiuw Chen, Xi Wang, and Xiang Bai. EPNet++: Cascade Bi-Directional Fusion for Multi-modal 3D Object Detection. *IEEE transactions on pattern analysis and machine intelligence*, 45(7):8324–8341, 2022.
- [19] Zhijian Liu, Haotian Tang, Alexander Amini, Xinyu Yang, Huizi Mao, Daniela L Rus, and Song Han. BEVfusion: Multi-task multi-sensor fusion with unified bird’s-eye view representation. In *2023 IEEE international conference on robotics and automation (ICRA)*, pages 2774–2781. IEEE, 2023.
- [20] Anas Mahmoud, Jordan SK Hu, and Steven L Waslander. Dense Voxel Fusion for 3D Object Detection. In *Proceedings of the IEEE/CVF winter conference on applications of Computer Vision*, pages 663–672, 2023.
- [21] Madhusri Maity, Sriparna Banerjee, and Sheli Sinha Chaudhuri. Faster R-CNN and YOLO based Vehicle Detection: A Survey. In *2021 5th international conference on computing methodologies and communication (ICCMC)*, pages 1442–1447. IEEE, 2021.
- [22] Gregory P Meyer, Ankit Laddha, Eric Kee, Carlos Vallespi-Gonzalez, and Carl K Wellington. LaserNet: An efficient probabilistic 3D object detector for Autonomous Driving. In *Proceedings of the IEEE/CVF conference on Computer Vision and Pattern Recognition*, pages 12677–12686, 2019.
- [23] Arsalan Mousavian, Dragomir Anguelov, John Flynn, and Jana Kosecka. 3D bounding box estimation using deep learning and geometry. In *Proceedings of the IEEE conference on Computer Vision and Pattern Recognition*, pages 7074–7082, 2017.
- [24] Vinod Nair and Geoffrey E. Hinton. Rectified linear units improve restricted boltzmann machines. In *Proceedings of the 27th International Conference on International Conference on Machine Learning, ICML’10*, page 807–814, Madison, WI, USA, 2010. Omnipress.
- [25] Su Pang, Daniel Morris, and Hayder Radha. CloCs: Camera-LiDAR object candidates fusion for 3D Object Detection. In *2020 IEEE/RSJ International Conference on Intelligent Robots and Systems (IROS)*, pages 10386–10393. IEEE, 2020.
- [26] Su Pang, Daniel Morris, and Hayder Radha. Fast-clocs: Fast Camera-LiDAR object candidates fusion for 3D Object Detection. In *Proceedings of the IEEE/CVF Winter Conference on Applications of Computer Vision*, pages 187–196, 2022.
- [27] Charles R Qi, Hao Su, Kaichun Mo, and Leonidas J Guibas. PointNet: Deep learning on Point sets for 3D classification and segmentation. In *Proceedings of the IEEE conference on Computer Vision and Pattern Recognition*, pages 652–660, 2017.
- [28] Charles Ruizhongtai Qi, Li Yi, Hao Su, and Leonidas J Guibas. PointNet++: Deep hierarchical feature learning on point sets in a metric space. *Advances in neural information processing systems*, 30, 2017.
- [29] LA Rakhsith, KS Anusha, BE Karthik, D Arun Nithish, and V Kishore Kumar. A Survey on Object Detection methods in Deep Learning. In *Proc. of 2021 Second Int. Conf. on Electronics and Sustainable Communication Systems (ICESC)*, 2021.
- [30] J Redmon. You Only Look Once: Unified, Real-Time Object Detection. In *Proceedings of the IEEE conference on Computer Vision and Pattern Recognition*, 2016.
- [31] Tahira Shehzadi, Khurram Azeem Hashmi, Didier Stricker, and Muhammad Zeshan Afzal. 2D Object Detection with Transformers: A Review. *arXiv preprint arXiv:2306.04670*, 2023.
- [32] Shaoshuai Shi, Chaoxu Guo, Li Jiang, Zhe Wang, Jianping Shi, Xiaogang Wang, and Hongsheng Li. PV-RCNN: Point-voxel feature set abstraction for 3DObject Detection. In *Proceedings of the IEEE/CVF conference on Computer Vision and Pattern Recognition*, pages 10529–10538, 2020.
- [33] Shaoshuai Shi, Xiaogang Wang, and Hongsheng Li. PointRCNN: 3D Object Proposal Generation and Detection from Point Cloud. In *Proceedings of the IEEE/CVF conference on Computer Vision and Pattern Recognition*, pages 770–779, 2019.
- [34] Pei Sun, Henrik Kretschmar, Xerxes Dotiwalla, Aurelien Chouard, Vijaysai Patnaik, Paul Tsui, James Guo, Yin Zhou, Yuning Chai, Benjamin Caine, et al. Scalability in perception for Autonomous Driving: Waymo open dataset. In *Proceedings of the IEEE/CVF*

conference on Computer Vision and Pattern Recognition, pages 2446–2454, 2020.

- [35] Sourabh Vora, Alex H Lang, Bassam Helou, and Oscar Beijbom. PointPainting: Sequential Fusion for 3D Object Detection. In *Proceedings of the IEEE/CVF conference on Computer Vision and Pattern Recognition*, pages 4604–4612, 2020.
- [36] Chunwei Wang, Chao Ma, Ming Zhu, and Xiaokang Yang. PointAugmenting: Cross-modal augmentation for 3D Object Detection. In *Proceedings of the IEEE/CVF conference on Computer Vision and Pattern Recognition*, pages 11794–11803, 2021.
- [37] Ke Wang, Tianqiang Zhou, Xingcan Li, and Fan Ren. Performance and challenges of 3D Object Detection methods in complex scenes for Autonomous Driving. *IEEE Transactions on Intelligent Vehicles*, 8(2):1699–1716, 2022.
- [38] Li Wang, Xinyu Zhang, Ziying Song, Jiangfeng Bi, Guoxin Zhang, Haiyue Wei, Liyao Tang, Lei Yang, Jun Li, Caiyan Jia, et al. Multi-modal 3D Object Detection in Autonomous Driving: A Survey and taxonomy. *IEEE Transactions on Intelligent Vehicles*, 8(7):3781–3798, 2023.
- [39] Xiangheng Wang, Hengyi Li, Xuebin Yue, and Lin Meng. A comprehensive Survey on Object Detection YOLO. *Proceedings http://ceur-ws.org ISSN*, 1613:0073, 2023.
- [40] Yan Wang, Wei-Lun Chao, Divyansh Garg, Bharath Hariharan, Mark Campbell, and Kilian Q Weinberger. Pseudo-LiDAR from visual depth estimation: Bridging the gap in 3D Object Detection for Autonomous Driving. In *Proceedings of the IEEE/CVF conference on Computer Vision and Pattern Recognition*, pages 8445–8453, 2019.
- [41] Zhangjing Wang, Yu Wu, and Qingqing Niu. Multi-Sensor Fusion in Automated Driving: A Survey. *IEEE Access*, 8:2847–2868, 2019.
- [42] Hai Wu, Chenglu Wen, Wei Li, Xin Li, Ruigang Yang, and Cheng Wang. Transformation-equivariant 3D Object Detection for Autonomous Driving. In *Proceedings of the AAAI Conference on Artificial Intelligence*, volume 37, pages 2795–2802, 2023.
- [43] Hai Wu, Chenglu Wen, Shaoshuai Shi, Xin Li, and Cheng Wang. Virtual Sparse Convolution for Multimodal 3D Object Detection. In *Proceedings of the IEEE/CVF Conference on Computer Vision and Pattern Recognition*, pages 21653–21662, 2023.
- [44] Xiaopei Wu, Liang Peng, Honghui Yang, Liang Xie, Chenxi Huang, Chengqi Deng, Haifeng Liu, and Deng Cai. Sparse Fuse Dense: Towards high quality 3D Detection with Depth Completion. In *Proceedings of the IEEE/CVF conference on Computer Vision and Pattern Recognition*, pages 5418–5427, 2022.
- [45] Zizhang Wu, Yuanzhu Gan, Lei Wang, Guilian Chen, and Jian Pu. MonoPGC: Monocular 3D Object Detection with pixel geometry contexts. In *2023 IEEE International Conference on Robotics and Automation (ICRA)*, pages 4842–4849. IEEE, 2023.
- [46] Shaoqing Xu, Dingfu Zhou, Jin Fang, Junbo Yin, Zhou Bin, and Liangjun Zhang. FusionPainting: Multimodal Fusion with Adaptive Attention for 3D Object Detection. In *2021 IEEE International Intelligent Transportation Systems Conference (ITSC)*, pages 3047–3054. IEEE, 2021.
- [47] Yan Yan, Yuxing Mao, and Bo Li. SECOND: Sparsely Embedded Convolutional Detection. *Sensors*, 18(10):3337, 2018.
- [48] Tianwei Yin, Xingyi Zhou, and Philipp Krähenbühl. Multimodal Virtual Point 3D Detection. *Advances in Neural Information Processing Systems*, 34:16494–16507, 2021.
- [49] Renrui Zhang, Han Qiu, Tai Wang, Ziyu Guo, Ziteng Cui, Yu Qiao, Hongsheng Li, and Peng Gao. MonoDETR: Depth-guided Transformer for Monocular 3D Object Detection. In *Proceedings of the IEEE/CVF International Conference on Computer Vision*, pages 9155–9166, 2023.
- [50] Tingyu Zhang, Zhigang Liang, Yanzhao Yang, Xinyu Yang, Yu Zhu, and Jian Wang. Contrastive Late Fusion for 3D Object Detection. *IEEE Transactions on Intelligent Vehicles*, 2024.
- [51] Xiangmo Zhao, Pengpeng Sun, Zhigang Xu, Haigen Min, and Hongkai Yu. Fusion of 3D LiDAR and Camera data for Object Detection in Autonomous Vehicle Applications. *IEEE Sensors Journal*, 20(9):4901–4913, 2020.
- [52] Yin Zhou and Oncel Tuzel. VoxelNet: End-to-end Learning for Point Cloud based 3D Object Detection. In *Proceedings of the IEEE conference on Computer Vision and Pattern Recognition*, pages 4490–4499, 2018.
- [53] Zhengxia Zou, Keyan Chen, Zhenwei Shi, Yuhong Guo, and Jieping Ye. Object Detection in 20 years: A Survey. *Proceedings of the IEEE*, 111(3):257–276, 2023.